Atmospheric Pollution Research 6 (2015) 562-571
Technical Note

Atmospheric Pollution Research

www.atmospolres.com

Spatiotemporal variability in dust observed over the Sinkiang and Inner Mongolia regions of Northern China

Hui Xu, Tianhai Cheng, Xingfa Gu, Tao Yu, Donghai Xie, Fengjie Zheng

State Key Laboratory of Remote Sensing Science, Institute of Remote Sensing and Digital Earth, Chinese Academy of Sciences, Beijing 100101, China

ABSTRACT

This study presents a detailed analysis of the spatiotemporal variability in dust observed over Sinkiang and Inner Mongolia in Northern China from 2005 to 2008. The relationships between airborne dust (observed by OMI–AI and MODIS–AOD), the normalized difference vegetation index (NDVI), monthly total precipitation (MTP) and surface wind speed (SWS) are investigated. The results show that the spatial distribution of airborne dust distinctly decreases from west to east across Northern China; this pattern is opposite to that of the NDVI and MTP. Both Sinkiang and Inner Mongolia experience high amounts of airborne dust in spring, with the highest values in April. The two regions also had different dust variabilities. In Sinkiang, three major dust regions were identified, with airborne dust mainly distributed in regions with NDVI values between 0 and 0.1, SWS values between 2 and 5 m/s, and a MTP of less than 5 mm. In addition, the temporal variation in airborne dust exhibits both positive and negative correlations with the NDVI, MTP and SWS. However, over Inner Mongolia, five high–dust regions were confirmed, with airborne dust generally distributed in the areas with NDVI values between 0 and 0.4, SWS values between 3 and 6 m/s, and a MTP of less than 10 mm. The time series of airborne dust is negatively correlated with the NDVI and MTP but strongly and positively correlated with the SWS. In addition, the temporal pattern of the AOD in Sinkiang is essentially controlled by dust activity, whereas it may be influenced by anthropogenic emissions in Inner Mongolia. Overall, the spatiotemporal variabilities in dust over Sinkiang and Inner Mongolia are not identical, although both regions are important sources of dust in East Asia.

Keywords: *Airborne dust, spatiotemporal variability, Northern China, AI and AOD*

Corresponding Author:
Tianhai Cheng
☎ : *+86-10-64839562*
🖷 : *+86-10-64839562*
✉ : *cthy@irsa.ac.cn*

Article History:
Received: 11 August 2014
Revised: 24 December 2014
Accepted: 24 December 2014

doi: 10.5094/APR.2015.063

1. Introduction

From west to east across Northern China, abundant dust activities occur annually over the arid and semi–arid areas (Zhang et al., 1997; Xuan et al., 2000; Natsagdorj et al, 2003; Wang et al., 2008). Airborne dust originating from these areas is frequently transported over vast regions of East Asia (Xuan and Sokolik, 2002; Zhang et al., 2003a; Shao and Dong, 2006) and is the cause of various hazards (health hazards and transportation system interference) that affect the livelihood of downwind residents. Furthermore, because of its complex direct (reducing surface insolation and heating atmospheric layers) and indirect (altering cloud properties and precipitation) effects on the state of the atmosphere and underlying surfaces (Levin et al., 1996; Miller and Tegen, 1998; Huang et al., 2006a; Huang et al., 2006b; Huang et al., 2006c), airborne dust is reportedly a key factor in climate systems (Haywood and Boucher, 2000). Accordingly, the distribution of dust and its changes are important to monitor, particularly over regions affected by frequent and intense dust activities, such as Sinkiang and Inner Mongolia in Northern China.

In recent decades, monitoring and analyzing dust events over Asia have progressed using various instruments. Among the measurements, ground–based observations appear to be the most logical candidates for airborne dust investigations (Darmenova et al., 2005) because their reported surface and meteorological parameters are key factors that govern the emission and transport of dust. For instance, using 174 Chinese weather stations, Sun et al. (2001) analyzed the spatiotemporal characteristics of dust storms in China from 1960 to 1999. Through an analysis of datasets derived from 83 Chinese weather stations, Qian et al. (2002) discovered a decrease in dust storms in China from 1954 to 1998. Wang et al. (2008) analyzed the variability in East Asian dust events and their long–term trends from 1954 to 2000 based on 701 meteorological stations. In addition, many valuable dust studies were also conducted during the Asia Pacific Regional Aerosol Characterization Experiment (ACE–Asia) in China, Korea, and Japan (Gong et al., 2003; Zhang et al., 2003b; Shimizu et al., 2004; Hsu et al., 2006; Kim et al., 2007).

Another approach to investigating airborne dust is to exploit satellite observations. Compared with ground–based measurements, satellite remote sensing has the distinct advantage of providing dust information at regional or even global scales. Thus, although satellite observations have larger uncertainties compared with ground–based measurements, they are still widely used to study the spatiotemporal and vertical variability in dust (Torres et al., 1998; Hsu et al., 2004; Huang et al., 2007; Hu et al., 2008; DeSouza–Machado et al., 2010; Kluser et al., 2011; Schepanski et al., 2012). For example, Darmenova et al. (2005) investigated the characteristics of spring dust outbreaks over East Asia by combining multi–sensor observations. Huang et al. (2008) analyzed the long–range transport and vertical structure of Asian dust based on Cloud–Aerosol Lidar and Infrared Pathfinder Satellite Observation (CALIPSO) measurements. Ginoux et al. (2012) presented a global–scale map of dust sources based on Moderate–resolution Imaging Spectroradiometer (MODIS) estimates of aerosol optical depth in conjunction with auxiliary datasets.

Although Asian dust activities have been thoroughly investigated through systematic measurements, few studies have assessed the similarities and differences in dust variability over

Sinkiang and Inner Mongolia, which are two important dust source regions in East Asia. Thus, a comprehensive comparison between the two regions is still lacking. Therefore, we monitored airborne dust over these areas, and our aim is to present the spatial distribution and temporal variation in dust using satellite imagery. Furthermore, this study examines the relationship between airborne dust and vegetation condition, precipitation and wind speed. The results of this study should be helpful in understanding the spatiotemporal variability in dust over Northern China. The paper is structured as follows: a description of the datasets and study areas is given in Section 2; a comprehensive analysis of airborne dust observed over Sinkiang and Inner Mongolia is conducted in Section 3; and the conclusions are presented in Section 4.

2. Datasets and Study Areas

2.1. Dataset descriptions

OMI Dust Aerosol Index (DAI). The Aerosol Index (AI) derived from the Ozone Monitoring Instrument (OMI) on board the Aura satellite is particularly suitable for detecting the presence of ultraviolet (UV) absorbing aerosols (dust, smoke, and volcanic ash) (Prospero et al., 2002; de Graaf et al., 2005). This index is defined as the difference between observations and model calculations of absorbing and non–absorbing spectral radiance ratios (Torres et al., 1998). Because of the low UV surface albedo of all ice–free and snow–free terrestrial surfaces and the high UV absorption of airborne dust, the AI has been widely used to monitor dust over a large variety of land surfaces (Yao et al., 2012), although it is also dependent on the altitude of the dust layer (Ginoux and Torres, 2003). To analyze the spatiotemporal variability in dust, the monthly dust aerosol index (DAI) is obtained by dividing the total AI values of all dust days per grid cell and month by the total number of days with satellite data availability. To eliminate signals contributed by background aerosols or other conditions, only AI values larger than 1.0 are considered as dust days in this study.

MODIS Aerosol Optical Depth (AOD). The Moderate–resolution Imaging Spectroradiometer (MODIS) sensors carried by the Terra/Aqua satellites were designed to improve our understanding of global dynamics. The MODIS aerosol products use three algorithms (Ocean, Dark Target, and Deep Blue) to monitor the ambient AOD over the global oceans and continents (Remer et al., 2005). The Deep Blue algorithm (Hsu et al., 2004) was developed to retrieve the AOD at 550 nm over bright land areas; the results in this band have been thoroughly compared with those derived from Aerosol Robotic Network (AERONET) over arid and semi–arid areas, and the results are consistent for a majority of sites (Ginoux et al., 2012). Compared with the OMI AI, MODIS AOD measurements are sensitive to both absorbing and non–absorbing aerosols.

MODIS Normalized Difference Vegetation Index (NDVI). The NDVI dataset derived from MODIS observations has been extensively used as an indicator of vegetation activity. The NDVI values are calculated from atmospherically corrected reflectance in the red and near–infrared bands (Huete et al., 2002). Generally, for surfaces covered with dense vegetation, the NDVI tends to have values close to 1.0. However, for surfaces with low vegetation cover or no vegetation cover, the NDVI values tend to be negative or close to –1.0.

GPCC Monthly Total Precipitation (MTP) and NCEP Surface Wind Speed (SWS). The Global Precipitation Climatology Centre (GPCC) Full V6 monthly total precipitation dataset and National Centers for Environment Prediction–Department of Energy (NCEP–DOE) Reanalysis 2 dataset (Kanamitsu et al., 2002) were investigated in this research because their monthly changes are critical for analyzing variations in airborne dust. Specifically, the monthly total precipitation dataset (unit: mm) is produced based on 67 200 worldwide ground–based stations. NCEP–DOE Reanalysis 2 contains multiple atmospheric variables at different altitudes. In this study, the 1 000 hPa surface wind speed (unit: m/s) was extracted from the NCEP–DOE Reanalysis 2 dataset.

Table 1 summarizes the detailed information on the above-mentioned datasets. For temporal and spatial consistency, all of the datasets were re–sampled to a uniform grid with a spatial resolution of 0.25 by 0.25 degrees using bilinear interpolation prior to the analysis. The data spanned January 1, 2005 to December 31, 2008.

2.2. Study areas

In spring, cyclonic activity associated with the Siberian and Mongolia Highs often induce strong winds over Sinkiang and Inner Mongolia (Liu et al., 2004; Shao and Dong, 2006), and blow massive sand and dirt particles into the atmosphere (Xuan and Sokolik, 2002; Wang et al., 2008). Furthermore, as controlled by the northerly and northwesterly middle tropospheric winds, airborne dust that originates from these areas is often transported east or southeast into Eastern China and possibly Korea and Japan, as shown in Figure 1. Therefore, to investigate the spatial and temporal variability in dust over Northern China, Sinkiang and Inner Mongolia were selected as the study areas.

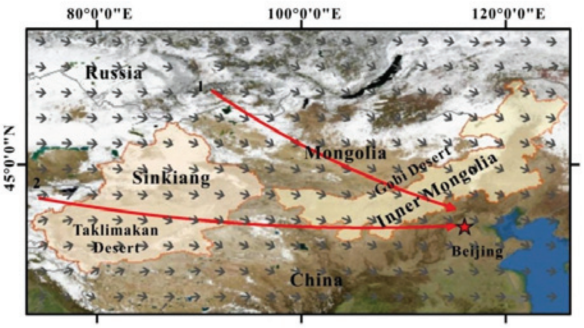

Figure 1. *Study region, including Sinkiang and Inner Mongolia. The red lines show the two major dust transmission paths in spring over Northern China, and the arrows denote the average 500–hPa wind direction over Northern China in spring from 2005 to 2008.*

3. Results and Discussion

3.1. Spatial distribution

In this section, the spatial distribution of airborne dust observed over Sinkiang and Inner Mongolia is analyzed. Figure 2 summarizes the spatial distribution maps of the annually averaged values of the DAI (Figure 2a) and AOD (Figure 2b). As presented in Figure 2, both the DAI and AOD exhibit pronounced spatial variability over Northern China, with western maxima and eastern minima. The DAI and AOD values observed over Inner Mongolia are lower than those observed over Sinkiang, which suggests that dust activity over Inner Mongolia is somewhat weaker than that of Sinkiang. The annual mean dust observations also reveal several hot–spot regions with values that are generally higher than their surrounding areas (marked by the numbers in Figure 2). Specifically, the highest DAI and AOD values are observed in Southern Sinkiang, particularly within the Taklamakan Desert, indicating that dust events over this area are much more frequent and severe than those over any other region of Sinkiang and Inner Mongolia. In Northern Sinkiang, the high DAI and AOD values are mainly concentrated in the Junggar Basin and Turpan Basin, which are both known as dust source regions in Sinkiang (Ginoux et al., 2012). In addition to the three high dust occurrence regions, other hot–spot regions with enhanced DAI and AOD values are observed from west to southeast of Inner Mongolia, such as in the Badain

Juran, Tengger and Mu Us Deserts in the west and the Otindag and Horqin sandy areas in the center and southeast. Because the occurrence of dust over a source region is assumed to be more frequent and intense than that over non–source regions (Schepanski et al., 2012), the airborne dust observed over Northern China probably originated from these distinctly arid and semi–arid areas.

Figure 3 shows the annual mean spatial distribution of the NDVI (Figure 3a), MTP (Figure 3b) and SWS (Figure 3c) over Sinkiang and Inner Mongolia. As shown in Figure 3, both the NDVI and MTP exhibit a reverse spatial variation pattern compared with the variation in airborne dust. High DAI and AOD areas generally correspond to regions with low NDVI and MTP values. Specifically, the annual mean DAI and AOD values observed over Northeastern Inner Mongolia are as low as 0.1 and 0.05, respectively, whereas the annual mean NDVI and MTP values in these areas are as high as 0.6 and 40 mm, respectively. However, the annual mean DAI and AOD values observed over Southern Sinkiang are nearly ten times higher than those observed over Northeastern Inner Mongolia, whereas the annual mean NDVI and MTP values in Southern Sinkiang are significantly lower than those of Northeastern Inner Mongolia. Large contrasts in the SWS are also observed from west to east across Northern China, as shown in Figure 3c. The relationship between the observed airborne dust and the SWS is not obvious, although the wind speed has been reported to be the driving force for dust emissions and transport (Natsagdorj et al., 2003; Liu et al., 2004; Shao and Dong, 2006). These results indicate that the spatial variation pattern of dust in Northern China is possibly governed by vegetation cover and precipitation instead of the surface wind speed.

Table 1. *Observational data sets used for the analyses in this study*

Type	Frequency	Spectral Resolution	Data Sources
Aerosol index	Daily	0.25×0.25	OMI http://giovanni.gsfc.nasa.gov
Aerosol optical depth	Monthly average	1.0×1.0	Aqua MODIS (Deep Blue) http://giovanni.gsfc.nasa.gov
Normalized difference vegetation index	Monthly average	0.05×0.05	Aqua MODIS https://lpdaac.usgs.gov/get_data/data_pool
Precipitation	Monthly total	0.5×0.5	GPCC http://www.esrl.noaa.gov/psd/data/gridded
Surface wind speed	Monthly average	2.5×2.5	NCEP-DOE Reanalysis 2 ftp.cdc.noaa.gov

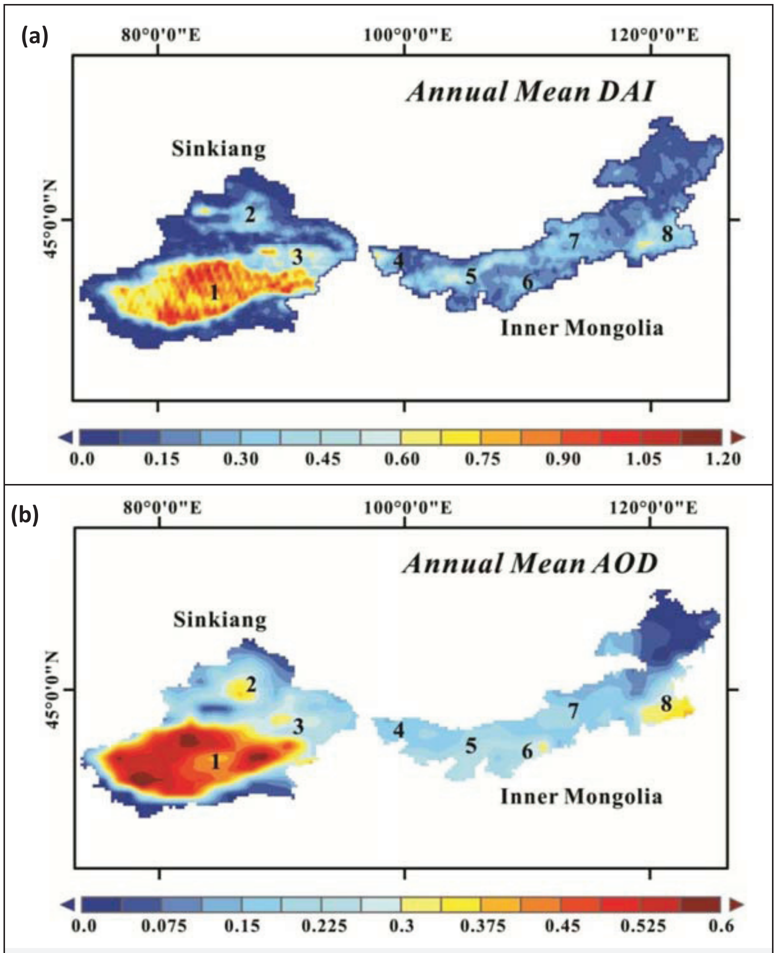

Figure 2. *Annual mean maps of the spatial distribution of the* ***(a)*** *DAI and* ***(b)*** *AOD values over Sinkiang and Inner Mongolia from 2005 to 2008.*

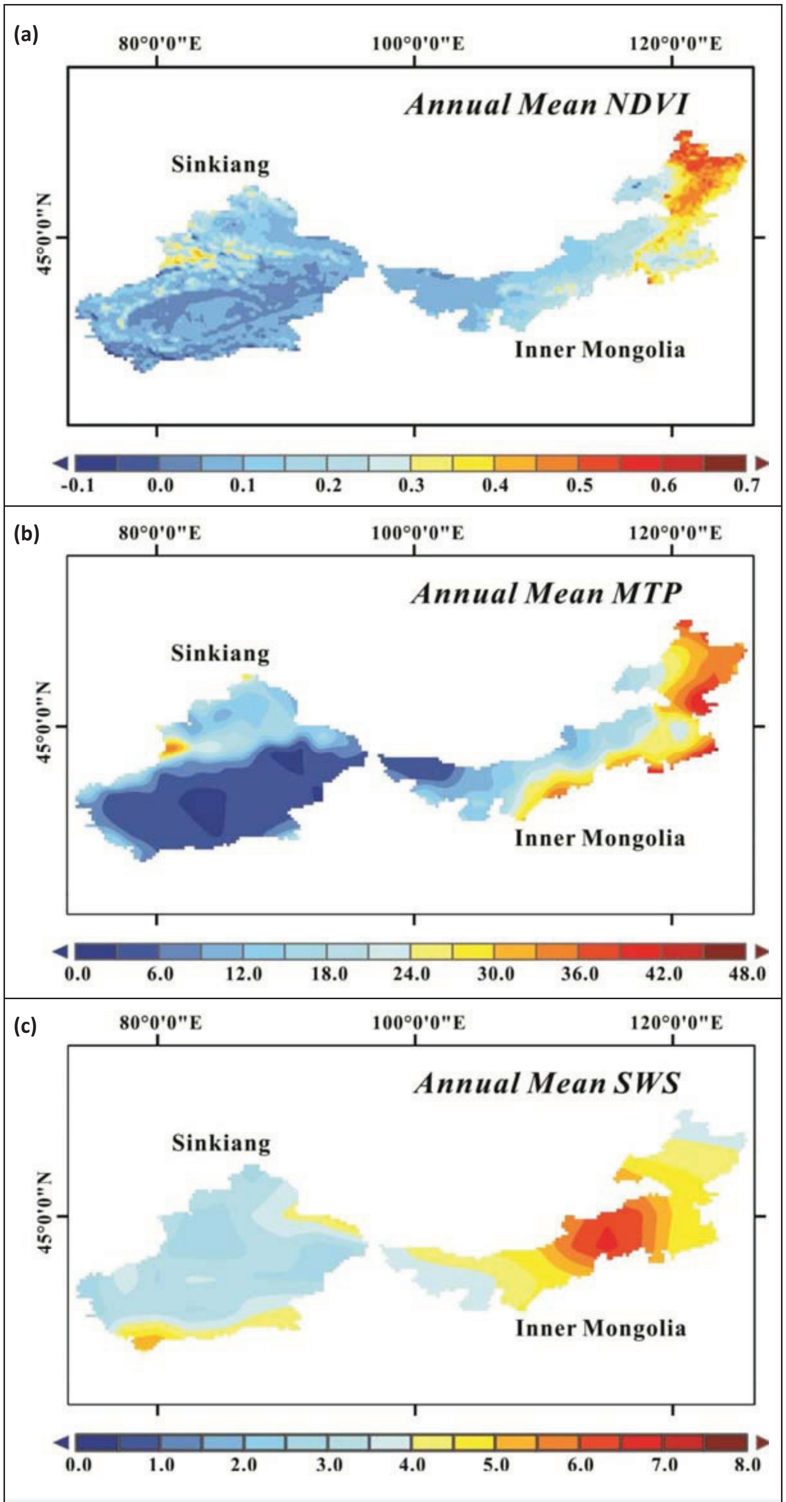

Figure 3. *Annual mean maps of the spatial distribution of the* ***(a)*** *NDVI,* ***(b)*** *MTP and* ***(c)*** *SWS over Sinkiang and Inner Mongolia from 2005 to 2008.*

Figure 4 shows the scatter plots of the DAI versus NDVI (Figure 4a), MTP (Figure 4b) and SWS (Figure 4c) based on the monthly observations (pixel value per month). In general, airborne dust observed over Sinkiang is mostly distributed in areas with NDVI values between 0 and 0.1, SWS values between 2 and 5 m/s, and MTP values less than 5 mm. Compared with those in Sinkiang, dust events in Inner Mongolia can be observed over a wide range of NDVI values (between 0 and 0.4). Additionally, when dust events occur over Inner Mongolia, the SWS and MTP values are generally less than 10 mm and approximately 3 to 6 m/s, respectively. These discrepancies are probably caused by differences in topography. As far from the ocean and surrounded by highlands on three sides (the Mongolian Plateau to the north, the Pamir Plateau to the west and the Tibetan Plateau to the south), Sinkiang has significantly lower moisture than the average in China. This lack of moisture leads to an extreme lack of precipitation, dry soil, and reduced plant life, thus, many areas become large deserts and provide abundant loose particles for dust emission. Therefore, in these areas, even a weak wind can lift massive amounts of sand and dirt particles off the ground. However, as closer to the Pacific Ocean, moisture from the ocean provides more precipitation to Inner Mongolia than to Sinkiang. This helps enhance soil moisture, vitalize the vegetation, and prevent soil erosion. Consequently, the wind speed over Inner Mongolia must exceed a threshold before it can lift particles at the ground. These results are consistent with the results presented by Wang et al. (2008).

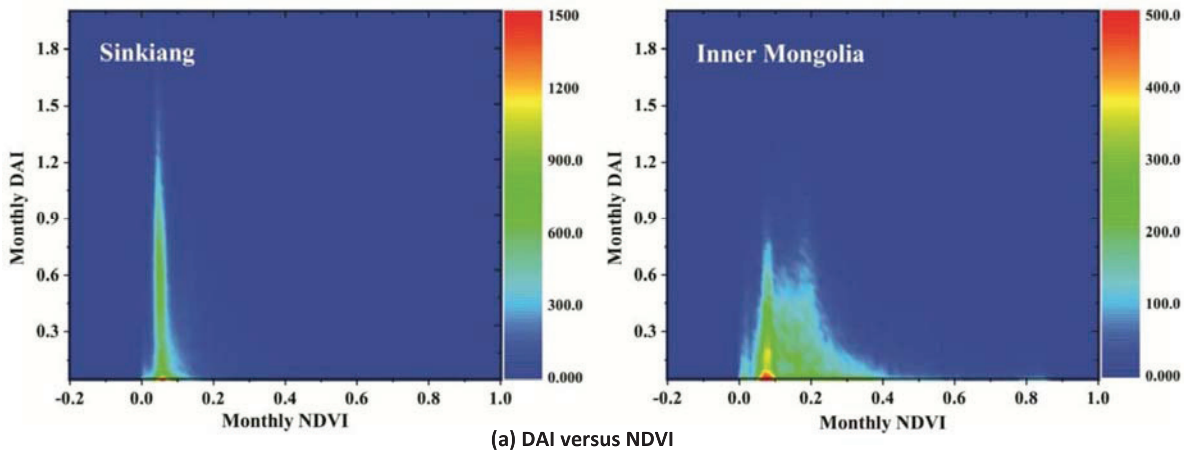

(a) DAI versus NDVI

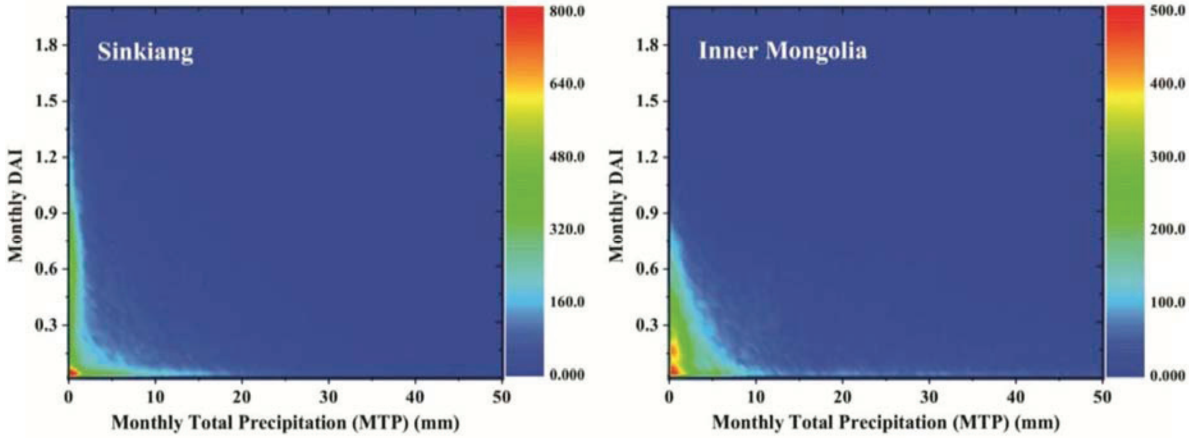

(b) DAI versus MTP

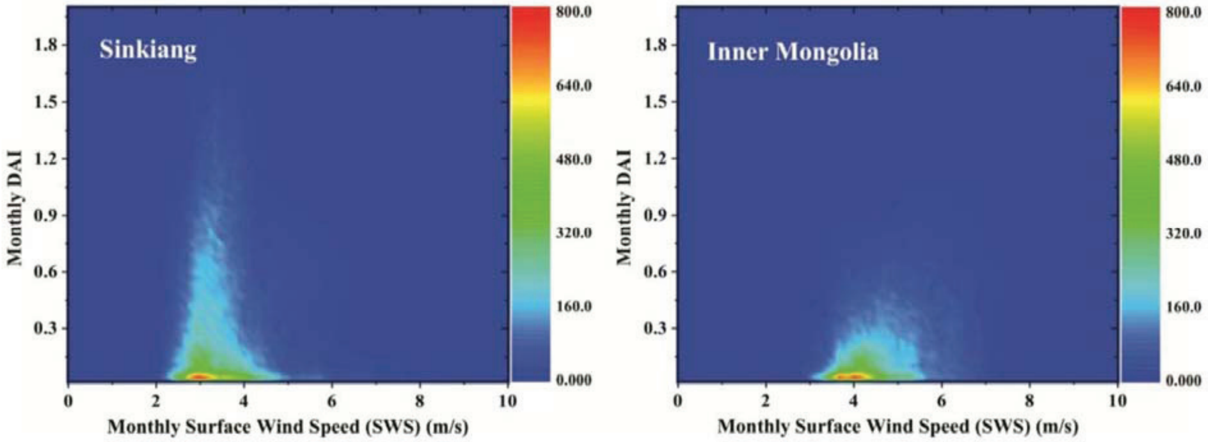

(c) DAI versus SWS

Figure 4. *Scatter plots of the DAI versus the* ***(a)*** *NDVI,* ***(b)*** *MTP and* ***(c)*** *SWS based on the monthly observations (pixel value per month) from 2005 to 2008. The color bar represents the number of points.*

3.2. Temporal variation

In this section, the intra–annual and multi–year fluctuations in airborne dust (DAI and AOD) over Sinkiang and Inner Mongolia are analyzed and compared. Figure 5 shows the intra–annual variability in DAI and AOD obtained from the regional annual mean observations. In both Sinkiang and Inner Mongolia, distinct maximum DAI and AOD were observed in spring (March, April and May), with the highest values in April. The dust activity weakens rapidly in summer (June, July and August) and increases again in winter (December, January and February). Both the DAI and AOD values exhibit a secondary peak over Sinkiang in August. Interestingly, the intra–annual variations in the DAI and AOD appear to be quite similar in Sinkiang; however, they are not consistent in Inner Mongolia from July to November. This inconsistency is probably caused by anthropogenic aerosols (such as sulfates, nitrates and carbonaceous particles). In Sinkiang, particularly in the southern region, aerosols are mainly composed of sand and dust particles, whereas the non–dust component is low because of the absence of large industrial and urban centers. Thus, the variability in the DAI and AOD is strongly governed by airborne dust. However, Inner Mongolia is a new and developing industrial province known for its rich resources. The emission of anthropogenic aerosols from various sources (such as fossil fuels and exhaust gas) is increasing because of the rapid industrialization. Therefore, a considerable portion of the AOD value may be attributable to non–dust aerosols (except in the dusty season), resulting in different intra–annual variations between the DAI and AOD.

Figure 6 summarizes the monthly mean spatial distribution of the DAI over Sinkiang and Inner Mongolia. In winter, the DAI values are generally low except for some particular regions. From March onward, high DAI values begin to disperse over a large area and cover nearly all of the Sinkiang and Inner Mongolia regions. During summer, the DAI significantly decreases over most of Inner Mongolia. From September to November, the DAI values in Sinkiang begin to decrease, with the lowest values in November. Based on Figure 6, the DAI values of the hot–spot regions (as depicted in Figure 2) are mostly higher than those in surrounding areas throughout the year, indicating that these areas are probably the main dust emission regions in Northern China.

The inter–annual variability in the DAI and AOD values over Sinkiang and Inner Mongolia, along with the variabilities in the NDVI, MTP and SWS, were also analyzed based on the regional monthly mean observations, as shown in Figure 7. In Sinkiang, the DAI and AOD values were relatively low in 2005. Subsequently, both values increased dramatically in the spring of 2006 and stabilized over the next three years. In Inner Mongolia, the DAI and AOD values exhibited an increase from 2005 to 2006 and subsequently decreased from 2006 to 2007. After that, the values increased again from 2007 to 2008. The NDVI and MTP time series display a generally consistent pattern of variation (maximum in summer and minimum in winter) in both Sinkiang and Inner Mongolia. This finding is most likely related to the Asian monsoon. In the summer, monsoon winds from the Pacific Ocean can transport large amounts of water vapor to the arid and semi–arid regions; thus, more precipitation and vegetation are observed during this period. However, the influence of the terrain significantly lowers the NDVI and MTP values of Sinkiang compared with those of Inner Mongolia, as previously illustrated. Interestingly, the NDVI and MTP annual data series are nearly the same for all 4 years in the Sinkiang and Inner Mongolia regions, whereas the SWS temporal variations in Sinkiang and Inner Mongolia are completely different. In Sinkiang, the SWS value is higher in winter than in the other seasons, whereas in Inner Mongolia, the peak SWS value is observed in the spring. Notably, the inter–annual variations in the DAI over Inner Mongolia are absolutely consistent with those of the SWS.

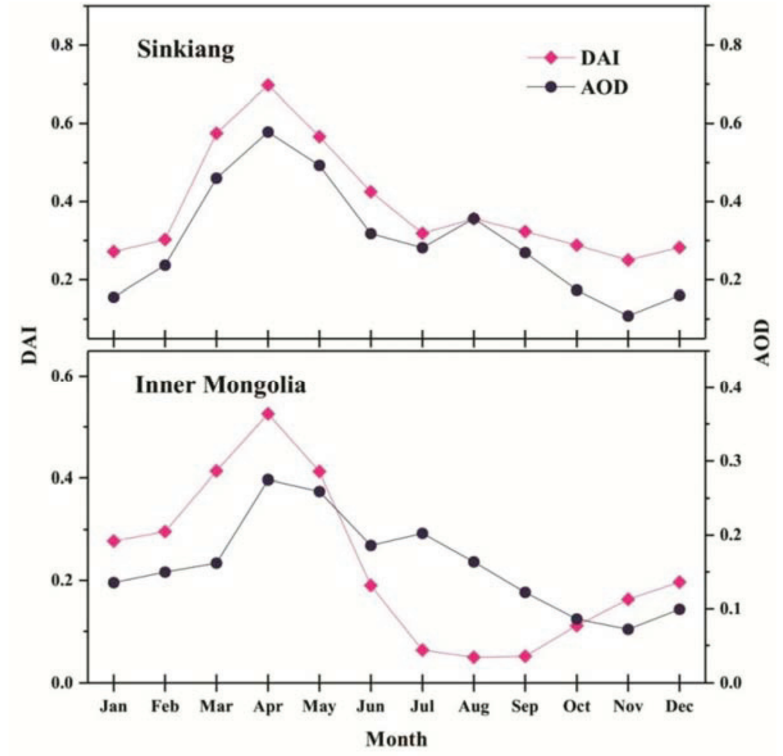

Figure 5. *The intra–annual variability in the DAI and AOD as obtained from the regional annual mean observations from 2005 to 2008.*

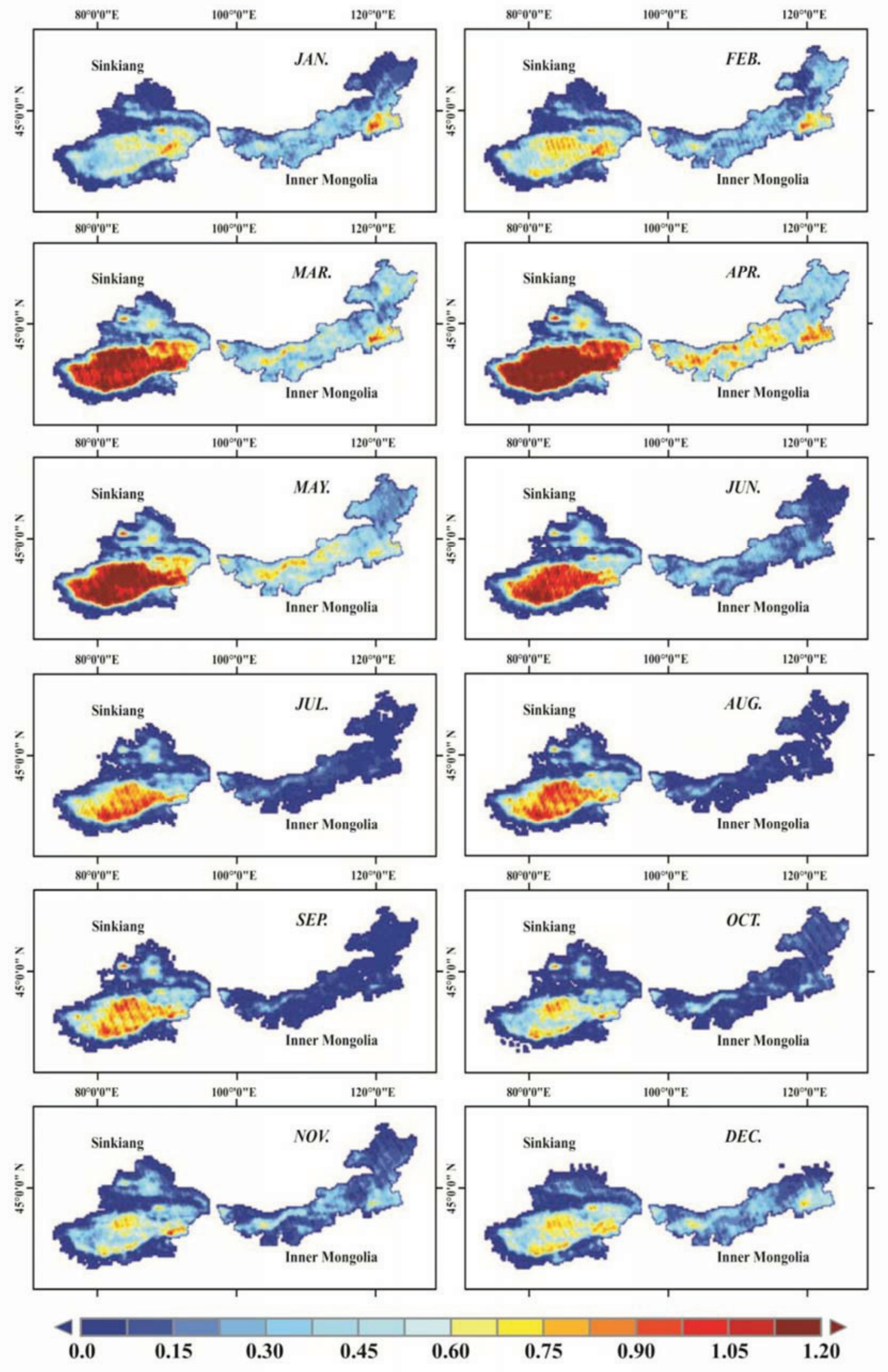

Figure 6. *Monthly mean spatial distribution of the DAI over Sinkiang and Inner Mongolia from 2005 to 2008.*

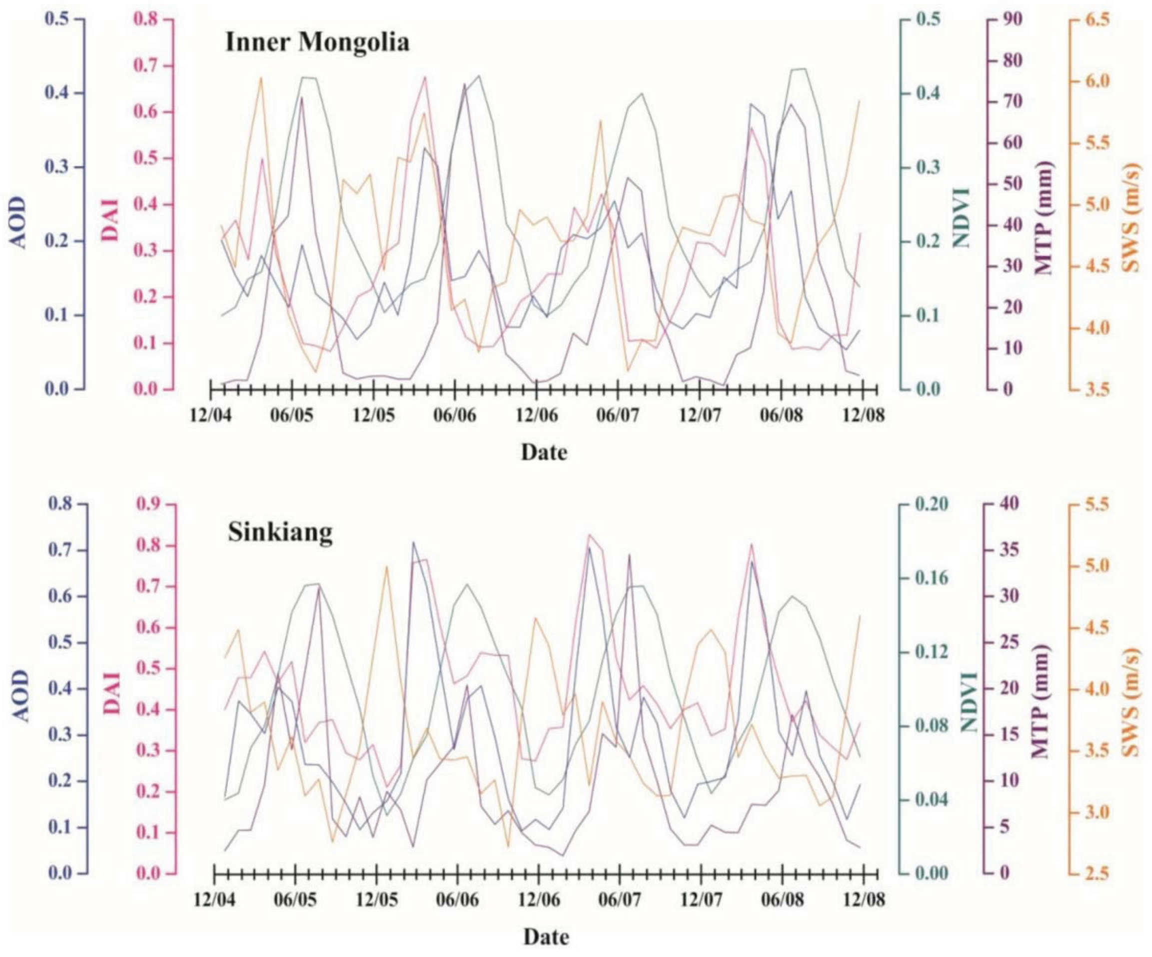

Figure 7. *The inter–annual variability in the DAI, AOD, NDVI, MTP and SWS as obtained from the regional monthly mean observations from 2005 to 2008.*

Based on the monthly observations, correlation coefficient maps of the DAI and NDVI (Figure 8a), MTP (Figure 8b) and SWS (Figure 8c) were obtained through correlation analysis. As shown in Figure 8, the DAI time series in Inner Mongolia is negatively correlated with the NDVI and MTP but strongly and positively correlated with the SWS. Thus, the temporal variation in airborne dust in Inner Mongolia is probably governed by vegetation coverage, precipitation and surface wind speed. Compared with that of Inner Mongolia, the temporal variation in the DAI in Sinkiang exhibits both positive and negative correlations with the NDVI, MTP and SWS. This indicates that the temporal variation in dust over Sinkiang is probably related to a more complex local climate system. In fact, dust events in the desert areas of Sinkiang are frequently caused by convective systems, in addition to the three factors mentioned here. Moreover, the mountain–valley breeze is an important factor for dust emissions in Sinkiang (Shao and Dong, 2006). Circulations in the severe arid basin create favorable conditions for suspending dust for a long time. Thus, the temporal variations in airborne dust over Sinkiang are complex relative to those in Inner Mongolia.

4. Conclusion

Satellite remote sensing provides valuable information for monitoring the spatiotemporal variability in airborne dust. In this study, airborne dust distribution patterns and variation trends were analyzed using multiple satellite observations (DAI from OMI and AOD from MODIS) in conjunction with useful auxiliary datasets (vegetation cover, monthly total precipitation and surface wind speed). Similarities and differences in dust variability over the arid and semi–arid areas of Northern China were revealed.

Airborne dust distinctly decreases from west to east across Northern China, and several high–dust occurrence regions were confirmed. Moreover, the spatial distribution of airborne dust is opposite to the distribution of vegetation cover and precipitation, rather than to surface wind speed. Thus, outbreaks of strong wind can only cause dust events over these areas when suitable dust emission condition occur. Dust activity observed over Northern China is higher in spring, with the highest values in April. The time series of airborne dust observed over Inner Mongolia is negatively correlated with vegetation cover and precipitation but strongly and positively correlated with surface wind speed. In Sinkiang, both positive and negative correlations between airborne dust and the three factors were obtained, indicating that dust emissions and transport over Sinkiang are more complex than those over Inner Mongolia. In addition, the temporal pattern of the AOD in Sinkiang is generally controlled by dust activities, whereas the AOD observed over Inner Mongolia remains high, even when dust activity is suppressed due to anthropogenic sources.

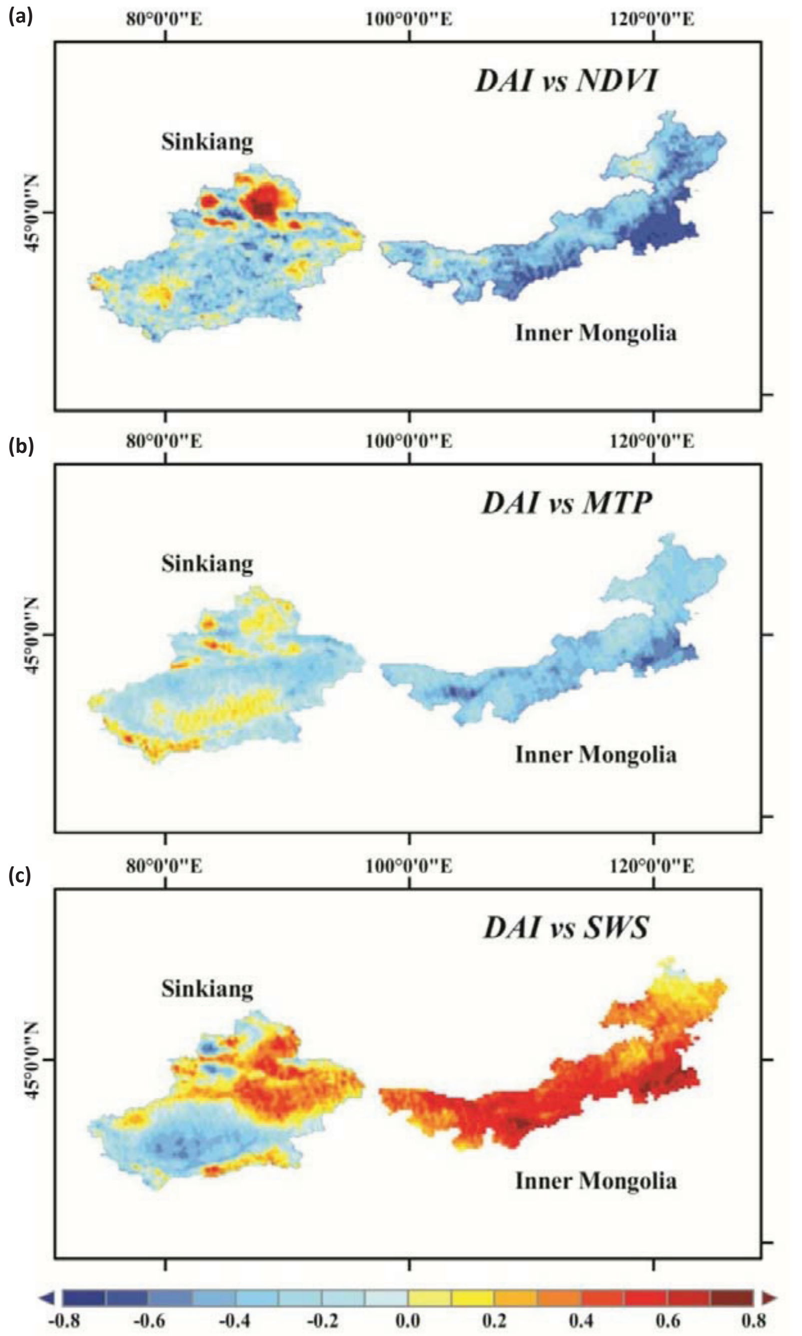

Figure 8. *Correlation coefficient maps of the spatial distribution between the DAI and the* ***(a)*** *NDVI,* ***(b)*** *MTP and* ***(c)*** *SWS over Sinkiang and Inner Mongolia, as calculated from the monthly observations (pixel value per month) from 2005 to 2008.*

Acknowledgments

This study was funded by the National Natural Science Foundation of China (No. 41401422, 41371015, 41001207) and Major State Basic Research Development Program of China (No. 2010CB950800). Additionally, the authors gratefully acknowledge GIOVANNI, Data Pool, GPCC and NCEP for providing the scientific remote sensing data. At last, the authors would like to specifically thank to anonymous reviewers for their constructive and valuable comments, which led to a significantly improved paper.

References

Darmenova, K., Sokolik, I.N., Darmenov, A., 2005. Characterization of East Asian dust outbreaks in the spring of 2001 using ground–based and satellite data. *Journal of Geophysical Research–Atmospheres* 110, art. no. D02204.

de Graaf, M., Stammes, P., Torres, O., Koelemeijer, R.B.A., 2005. Absorbing Aerosol Index: Sensitivity analysis, application to GOME and comparison with TOMS. *Journal of Geophysical Research–Atmospheres* 110, art. no. D01201.

DeSouza–Machado, S.G., Strow, L.L., Imbiriba, B., McCann, K., Hoff, R.M., Hannon, S.E., Martins, J.V., Tanre, D., Deuze, J.L., Ducos, F., Torres, O., 2010. Infrared retrievals of dust using AIRS: Comparisons of optical depths and heights derived for a North African dust storm to other collocated EOS A–Train and surface observations. *Journal of Geophysical Research–Atmospheres* 115, art. no. D15201.

Ginoux, P., Torres, O., 2003. Empirical TOMS index for dust aerosol: Applications to model validation and source characterization. *Journal of Geophysical Research–Atmospheres* 108, art. no. 4534.

Ginoux, P., Prospero, J.M., Gill, T.E., Hsu, N.C., Zhao, M., 2012. Global–scale attribution of anthropogenic and natural dust sources and their emission rates based on MODIS Deep Blue aerosol products. *Reviews of Geophysics* 50, art. no. RG3005.

Gong, S.L., Zhang, X.Y., Zhao, T.L., McKendry, I.G., Jaffe, D.A., Lu, N.M., 2003. Characterization of soil dust aerosol in China and its transport and distribution during 2001 ACE–Asia: 2. Model simulation and validation. *Journal of Geophysical Research–Atmospheres* 108, art. no. 4262.

Haywood, J., Boucher, O., 2000. Estimates of the direct and indirect radiative forcing due to tropospheric aerosols: A review. *Reviews of Geophysics* 38, 513–543.

Hsu, N.C., Tsay, S.C., King, M.D., Herman, J.R., 2006. Deep blue retrievals of Asian aerosol properties during ACE–Asia. *IEEE Transactions on Geoscience and Remote Sensing* 44, 3180–3195.

Hsu, N.C., Tsay, S.C., King, M.D., Herman, J.R., 2004. Aerosol properties over bright–reflecting source regions. *IEEE Transactions on Geoscience and Remote Sensing* 42, 557–569.

Hu, X.Q., Lu, N.M., Niu, T., Zhang, P., 2008. Operational retrieval of Asian sand and dust storm from FY–2C geostationary meteorological satellite and its application to real time forecast in Asia. *Atmospheric Chemistry and Physics* 8, 1649–1659.

Huang, J., Minnis, P., Chen, B., Huang, Z.W., Liu, Z.Y., Zhao, Q.Y., Yi, Y.H., Ayers, J.K., 2008. Long–range transport and vertical structure of Asian dust from CALIPSO and surface measurements during PACDEX. *Journal of Geophysical Research–Atmospheres* 113, art. no. D23212.

Huang, J.P., Ge, J.M., Weng, F.Z., 2007. Detection of Asia dust storms using multisensor satellite measurements. *Remote Sensing of Environment* 110, 186–191.

Huang, J.P., Lin, B., Minnis, P., Wang, T.H., Wang, X., Hu, Y.X., Yi, Y.H., Ayers, J.K., 2006a. Satellite–based assessment of possible dust aerosols semi–direct effect on cloud water path over East Asia. *Geophysical Research Letters* 33, art. no. L19802.

Huang, J.P., Wang, Y.J., Wang, T.H., Yi, Y.H., 2006b. Dusty cloud radiative forcing derived from satellite data for middle latitude regions of East Asia. *Progress in Natural Science* 16, 1084–1089.

Huang, J.P., Minnis, P., Lin, B., Wang, T.H., Yi, Y.H., Hu, Y.X., Sun–Mack, S., Ayers, K., 2006c. Possible influences of Asian dust aerosols on cloud properties and radiative forcing observed from MODIS and CERES. *Geophysical Research Letters* 33, art. no. L06824.

Huete, A., Didan, K., Miura, T., Rodriguez, E.P., Gao, X., Ferreira, L.G., 2002. Overview of the radiometric and biophysical performance of the MODIS vegetation indices. *Remote Sensing of Environment* 83, 195–213.

Kanamitsu, M., Ebisuzaki, W., Woollen, J., Yang, S.K., Hnilo, J.J., Fiorino, M., Potter, G.L., 2002. NCEP–DOE AMIP–II reanalysis (R–2). *Bulletin of the American Meteorological Society* 83, 1631–1643.

Kim, J., Jung, C.H., Choi, B.C., Oh, S.N., Brechtel, F.J., Yoon, S.C., Kim, S.W., 2007. Number size distribution of atmospheric aerosols during ACE–Asia dust and precipitation events. *Atmospheric Environment* 41, 4841–4855.

Kluser, L., Martynenko, D., Holzer–Popp, T., 2011. Thermal infrared remote sensing of mineral dust over land and ocean: A spectral SVD based retrieval approach for IASI. *Atmospheric Measurement Techniques* 4, 757–773.

Levin, Z., Ganor, E., Gladstein, V., 1996. The effects of desert particles coated with sulfate on rain formation in the Eastern Mediterranean. *Journal of Applied Meteorology* 35, 1511–1523.

Liu, X.D., Yin, Z.Y., Zhang, X.Y., Yang, X.C., 2004. Analyses of the spring dust storm frequency of Northern China in relation to antecedent and concurrent wind, precipitation, vegetation, and soil moisture conditions. *Journal of Geophysical Research–Atmospheres* 109, art. no. D16210.

Miller, R.L., Tegen, I., 1998. Climate response to soil dust aerosols. *Journal of Climate* 11, 3247–3267.

Natsagdorj, L., Jugder, D., Chung, Y.S., 2003. Analysis of dust storms observed in Mongolia during 1937–1999. *Atmospheric Environment* 37, 1401–1411.

Prospero, J.M., Ginoux, P., Torres, O., Nicholson, S.E., Gill, T.E., 2002. Environmental characterization of global sources of atmospheric soil dust identified with the Nimbus 7 Total Ozone Mapping Spectrometer (TOMS) absorbing aerosol product. *Reviews of Geophysics* 40, art. no. 1002.

Qian, W.H., Quan, L.S., Shi, S.Y., 2002. Variations of the dust storm in China and its climatic control. *Journal of Climate* 15, 1216–1229.

Remer, L.A., Kaufman, Y.J., Tanre, D., Mattoo, S., Chu, D.A., Martins, J.V., Li, R.R., Ichoku, C., Levy, R.C., Kleidman, R.G., Eck, T.F., Vermote, E., Holben, B.N., 2005. The MODIS aerosol algorithm, products, and validation. *Journal of the Atmospheric Sciences* 62, 947–973.

Schepanski, K., Tegen, I., Macke, A., 2012. Comparison of satellite based observations of Saharan dust source areas. *Remote Sensing of Environment* 123, 90–97.

Shao, Y., Dong, C.H., 2006. A review on East Asian dust storm climate, modelling and monitoring. *Global and Planetary Change* 52, 1–22.

Shimizu, A., Sugimoto, N., Matsui, I., Arao, K., Uno, I., Murayama, T., Kagawa, N., Aoki, K., Uchiyama, A., Yamazaki, A., 2004. Continuous observations of Asian dust and other aerosols by polarization lidars in China and Japan during ACE–Asia. *Journal of Geophysical Research–Atmospheres* 109, art. no. D19S17.

Sun, J.M., Zhang, M.Y., Liu, T.S., 2001. Spatial and temporal characteristics of dust storms in China and its surrounding regions, 1960–1999: Relations to source area and climate. *Journal of Geophysical Research–Atmospheres* 106, 10325–10333.

Torres, O., Bhartia, P.K., Herman, J.R., Ahmad, Z., Gleason, J., 1998. Derivation of aerosol properties from satellite measurements of backscattered ultraviolet radiation: Theoretical basis. *Journal of Geophysical Research–Atmospheres* 103, 17099–17110.

Wang, X., Huang, J.P., Ji, M.X., Higuchi, K., 2008. Variability of East Asia dust events and their long–term trend. *Atmospheric Environment* 42, 3156–3165.

Xuan, J., Sokolik, I.N., 2002. Characterization of sources and emission rates of mineral dust in Northern China. *Atmospheric Environment* 36, 4863–4876.

Xuan, J., Liu, G.L., Du, K., 2000. Dust emission inventory in Northern China. *Atmospheric Environment* 34, 4565–4570.

Yao, Z.G., Li, J., Han, H.J., Huang, A.L., Sohn, B.J., Zhang, P., 2012. Asian dust height and infrared optical depth retrievals over land from hyperspectral longwave infrared radiances. *Journal of Geophysical Research–Atmospheres* 117, art. no. D19202.

Zhang, X.Y., Gong, S.L., Zhao, T.L., Arimoto, R., Wang, Y.Q., Zhou, Z.J., 2003a. Sources of Asian dust and role of climate change versus desertification in Asian dust emission. *Geophysical Research Letters* 30, art. no. 2272.

Zhang, X.Y., Gong, S.L., Shen, Z.X., Mei, F.M., Xi, X.X., Liu, L.C., Zhou, Z.J., Wang, D., Wang, Y.Q., Cheng, Y., 2003b. Characterization of soil dust aerosol in China and its transport and distribution during 2001 ACE–Asia: 1. Network observations. *Journal of Geophysical Research–Atmospheres* 108, art. no. 4261.

Zhang, X.Y., Arimoto, R., An, Z.S., 1997. Dust emission from Chinese desert sources linked to variations in atmospheric circulation. *Journal of Geophysical Research–Atmospheres* 102, 28041–28047.